J. Phys. Chem. A **2003,** *107,* 8949−8954

An ab Initio and AIM Study on the Molecular Structure and Stability of Small $Cu_xS_y^-$ Clusters

Boris Ni and James R. Kramer

School of Geography and Geology, McMaster University, Hamilton, Ontario, Canada

Nick H. Werstiuk*

Department of Chemistry, McMaster University, Hamilton, Ontario, Canada

Received: May 30, 2003; In Final Form: July 25, 2003

The molecular structure of small $Cu_xS_y^-$ anionic clusters, some of which are odd-electron species, was studied by combination of ab initio and atoms-in-molecules (AIM) calculations. It is found that covalent Cu−Cu bonding is weak, unstable and often is not realized, even though interatomic distances are found to be within the normal Cu−Cu bond range. Three new stable $Cu_xS_y^-$ clusters are revealed. On the basis of the structure of the new isomers, the relationship between reactivity of $Cu_xS_y^-$ ions with P_4 and coordination of sulfur atoms in the clusters is established.

Introduction

Copper−sulfide molecular clusters play an important role in inorganic and organic chemical processes. For example copper−sulfide clusters serve as catalytic centers in biologically important reactions of charge transfer, ligand exchange, and oxidative degradation.[1−4] Compounds containing CuS clusters are used in optoelectronic devices, photocatalysts and semiconductors.[5−8] New methods of growing Cu_2S nanowires show promise in generating new materials.[9−10] Despite the importance of these species, especially in the chemistry of natural organic matter, a detailed theoretical understanding of the molecular structure—the bonding—of the sulfide cluster complexes, the mechanisms of their reactions, and factors that control their stability is lacking. Accurate computational modeling of metal−sulfides is challenging even for relatively small clusters due to the large number of electrons involved. Recently, the experimental and computational studies of small of $(Cu_2S)_n$[11−14] and $Cu_xS_y^-$ anionic clusters[15−17] have been reported. In our previous investigation[14] we showed that the degree of covalent bonding in $(Cu_2S)_n$ and their stability can be overestimated if the bonding is assumed or assigned on the basis of interatomic distances. The purpose of this ab initio and AIM (atoms in molecules) study was to extend our reseah on the molecular structure—the bonding—and reactivity of copper sulfide clusters. The anionic clusters $(Cu_xS_y)^-$ that are the subject of this paper are of particular interest because they have been generated and their reactivities studied with P_4 in the gas phase.[15−17]

Computations

Equilibrium optimized geometries were obtained with DFT and perturbation-theory methods as implemented in GAUSSIAN 98.[18] DFT calculations were carried out at the Becke3PW91/6-311+G(d) level that includes the Becke−Perdew−Wang (Becke3PW91) exchange-correlation potential.[19] Perturbation-theory Möller−Plesset[20] calculations were carried out at the MP2(FC) frozen core level with the 6-311+G(d) basis set. The odd-electron species $Cu_2S_2^-$, $Cu_2S_3^-$, $Cu_4S_3^-$, and $Cu_6S_4^-$ were studied at the unrestricted levels UBecke3PW91 and UMP2-(FC).[20] Inclusion of polarization and diffuse functions was shown to be important[21] in calculations involving transition metals at correlated levels. Optimizations were performed in stages in the case of $Cu_2S_3^-$ (**4**) and larger clusters. Initial geometries were obtained with the MM+ force field of HyperChem,[22] with the molecular symmetries being set at this stage. In the next step, optimizations were carried out at both Becke3PW91 and MP2 levels with the 6-31G basis set with the SCF convergence criterion initially set to 10^{-6} and a virtual orbital shift of 0.6 au applied. In most cases, it was necessary to increase the SCF iteration limit to 300. After an optimized geometry was obtained at this level, a refined geometry was obtained at the 6-311+G(d) level with the SCF convergence criterion set to 10^{-7}. Single point calculations with SCF=TIGHT were used to obtain wave functions that were analyzed with the AIMPAC suite of programs[23] and AIM2000.[24] Wave function stability was verified at the Becke3PW91 level using the appropriate keywords: Stable=Opt and Guess (Read, Mix). Molecular graphs were obtained with AIM2000 and are displayed in Figures 1−4. To increase the accuracy of the energies calculated at the perturbation-theory level, higher order MP3 and MP4(SDQ) calculations were performed with the MP2 geometry. Where possible, we took advantage of the molecular symmetry to decrease computational time. However, in the case of $Cu_3S_3^-$ (**5**) and $Cu_6S_4^-$ (**7**) calculations on the highest symmetry structures failed, and symmetry was reduced to achieve convergence. In these cases, structures close to those expected for the high-symmetry species were obtained with the differences in interatomic distances being less than 0.06 Å.

Results and Discussion

Selected geometrical parameters of CuS_2^- (**1**), CuS_3^- (**2**), $Cu_2S_2^-$ (**3**), $Cu_2S_3^-$ (**4**), its isomer i-$Cu_2S_3^-$ (**i-4**), $Cu_3S_3^-$ (**5**) its isomer i-$Cu_3S_3^-$ (**i-5**), $Cu_4S_3^-$ (**6**), $Cu_5S_4^-$ (**7**), its isomer i-$Cu_5S_4^-$ (**i-7**), and $Cu_6S_5^-$ (**8**) are collected in Table 1. Overall,

---

* To whom correspondence should be addressed. E-mail: werstiuk@mcmaster.ca.

10.1021/jp035513h CCC: $25.00

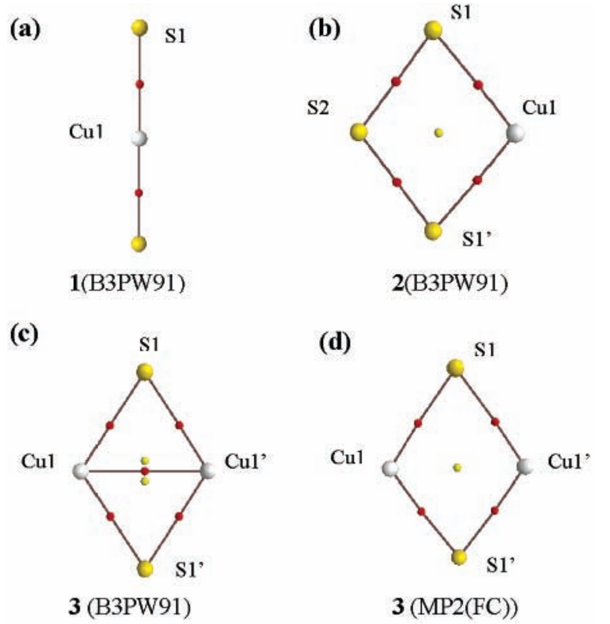

1(B3PW91) 2(B3PW91) 3 (B3PW91) 3 (MP2(FC))

Figure 1. Displays of molecular graphs: (a) **1** (CuS_2^-), (b) **2** (CuS_3^-), (c) **3** ($Cu_2S_2^-$) at Becke3PW91/6-311+G(d), and (d) **3** ($Cu_2S_2^-$) at MP2-(FC)/6-311+G(d). Copper atoms are shown as gray spheres, sulfur atoms as yellow spheres, bond critical points as small red spheres, and ring critical points as small yellow spheres.

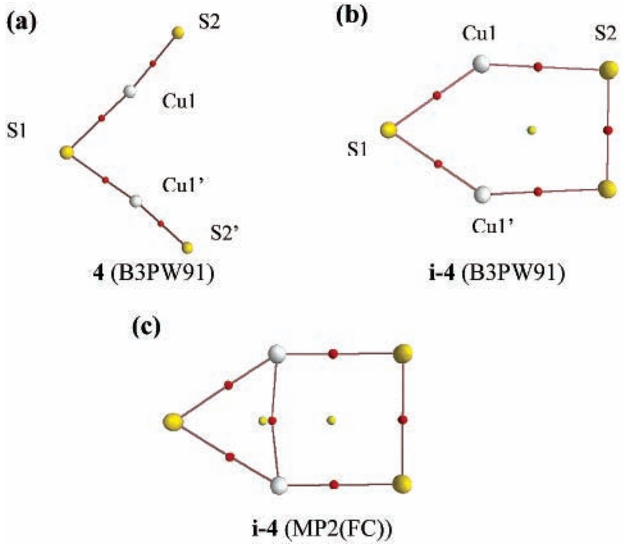

4 (B3PW91) i-4 (B3PW91) i-4 (MP2(FC))

Figure 2. Displays of molecular graphs: (a) **4** ($Cu_2S_3^-$), (b) **i-4** ($Cu_2S_3^-$) at Becke3PW91/6-311+G(d), and (c) **i-4** ($Cu_2S_3^-$) at MP2-(FC)/6-311+G(d). Copper atoms are shown as gray spheres, sulfur atoms as yellow spheres, bond critical points as small red spheres, and ring critical points as small yellow spheres.

the geometry of the clusters obtained at the Becke3PW91 and MP2(FC)—given in parentheses—levels are similar with the differences in internuclear distances obtained at these levels being less than 0.1 Å in most cases. The molecular structures of clusters as defined by the molecular graphs—in some cases at both levels—are presented in Figures 1−4; red spheres show the bond critical points (BCPs), small yellow spheres are ring critical points (RCPs), and the green spheres are cage critical points. The values of electron density $\rho(r_c)$ at the Cu−S and Cu−Cu BCPs are collected in Table 2. Bader[25] has used the values of $\rho(r_c)$ at BCPs and its Laplacian ($\nabla^2\rho$) to classify bonding interactions that are produced by sharing of electrons in covalent homo- and heteronuclear polar bonds. On the basis of the values of $\rho(r_c)$ (Table 2), and $\nabla^2\rho(r_c)$ (Table 3) and our previous investigation of copper(I) sulfide clusters,[14] the Cu−S and Cu−Cu bonds belong in the intermediate category with the Cu−S bonds having more covalent character than the Cu−Cu bonds. In both cases $\nabla^2\rho(r)$ is negative, whereas $\rho(r_c)$ is larger for the Cu−S than for Cu−Cu bonds (see Table 2). The magnitude of $\rho(r_c)$ for the similar kind of bonds depends on bond length and coordination of the atoms. Therefore the value of $\rho(r_c)$ is often used as a measure of the bond strength.[14,25] It is of interest to compare Cu−Cu and Cu−S bond strengths of the $Cu_xS_y^-$ and $(Cu_2S)_n$ clusters studied previously.[14] Yet this is not a simple matter because the clusters possess different ratios of Cu and S atom and exhibit different degrees of coordination.

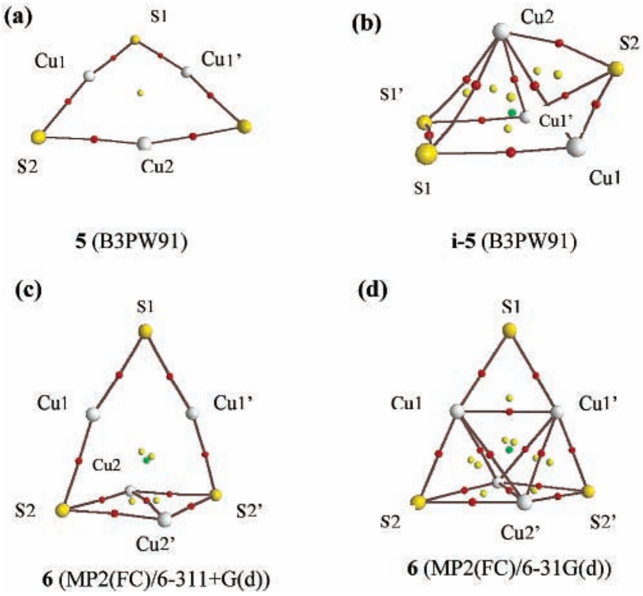

5 (B3PW91) i-5 (B3PW91) 6 (MP2(FC)/6-311+G(d)) 6 (MP2(FC)/6-31G(d))

Figure 3. Displays of molecular graphs: (a) **5** ($Cu_3S_3^-$), (b) **i-5** ($Cu_2S_3^-$) at Becke3PW91/6-311+G(d), (c) **6** ($Cu_4S_3^-$) at MP2(FC)/6-311+G(d), and (d) **6** ($Cu_4S_3^-$) at MP2(FC)/6-31G(d). Copper atoms are shown as gray spheres, sulfur atoms as yellow spheres, bond critical points as small red spheres, ring critical points as small yellow spheres, and cage critical points as green spheres.

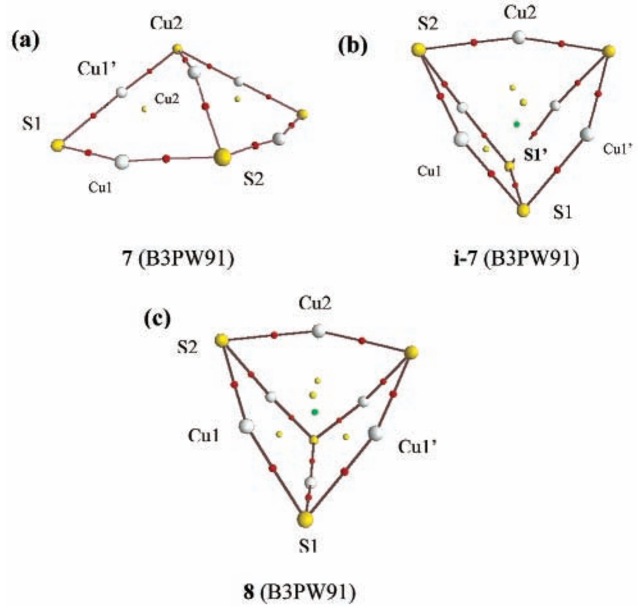

7 (B3PW91) i-7 (B3PW91) 8 (B3PW91)

Figure 4. Displays of molecular graphs: (a) **7** ($Cu_5S_4^-$), (b) **i-7** ($Cu_5S_4^-$), and (c) **8** ($Cu_6S_4^-$) at Becke3PW91/6-311+G(d). Copper atoms are shown as gray spheres, sulfur atoms as yellow spheres, bond critical points as small red spheres, ring critical points as small yellow spheres, and cage critical points as green spheres.

TABLE 1: Selected Internuclear Distances (Å) of $(Cu_xS_y)^-$ Clusters

cluster		S1−Cu1	Cu1−S2	S1−S2	S1−Cu2	S2−Cu2	Cu1−Cu1′	Cu1−Cu2	Cu1−Cu3	Cu2−Cu2′
1	CuS_2^-	2.071 (2.047)[b]								
2	CuS_3^-	2.217 (2.157)	2.692 (2.620)	2.172 (2.175)						
3	$Cu_2S_2^-$	2.210 (2.194)					2.430 (2.685)			
4	$Cu_2S_3^-$	2.134 (2.105)	2.092 (2.095)				2.736 (2.967)			
i-4[a]	$Cu_2S_3^-$ [a]	2.194 (2.137)	2.237 (2.134)	2.062 (2.186)			2.403 (2.292)			
5	$Cu_3S_3^-$	2.144 (2.088)	2.131 (2.077)				2.654 (2.606)	2.609 (2.558)		
i-5[a]	$Cu_3S_3^-$ [a]	2.252 (2.188)	2.241 (2.177)		2.515 (2.450)	2.423 (2.471)	2.585 (2.531)	2.396 (2.365)		
6	$Cu_4S_3^-$	2.181 (2.133)	2.212 (2.127)			2.277 (2.282)	2.413 (2.532)	2.734 (2.678)		2.440 (2.308)
7	Cu_5S_4	2.151 (2.109)	2.187 (2.137)			2.302 (2.238)	2.636 (2.547)	2.548 (2.540)		
i-7[a]	$Cu_5S_4^-$ [a]	2.254 (2.192)	2.241 (2.191)			2.237 (2.187)	2.665 (2.615)	2.665 (2.621)	2.439 (2.403)	
8	$Cu_6S_4^-$	2.232 (2.163)	2.213 (2.203)				2.671 (2.670)	2.675 (2.613)		

[a] The new clusters found. [b] The values in parentheses obtained at the MP2(FC)/6-311+G(d) level.

TABLE 2: Values of $\rho(r_c)$ (e Å^{-3}) at Bond Critical Points

cluster		S1−Cu1	Cu1−S2	S1−S2	S1−Cu2	S2−Cu2	Cu1−Cu1′	Cu1−Cu2	Cu1− Cu3	Cu2−Cu2′
1	CuS_2^-	0.516 (0.803)[b]								
2	CuS_3^-	0.550 (0.622)		0.762 (0.746)						
3	$Cu_2S_2^-$	0.567 (0.595)					0.313			
4	$Cu_2S_3^-$	0.663 (0.828)	0.723 (0.783)							
i-4[a]	$Cu_2S_3^-$	0.576 (0.669)	0.531 (0.684)	0.939 (0.722)			(0.406)			
5	$Cu_3S_3^-$	0.508 (0.557)	0.530 (0.711)			0.508 (0.441)				
i-5[a]	$Cu_3S_3^-$	0.464 (0.558)	0.436 (0.515)		0.262 (0.332)	0.335 (0.345)				
6	$Cu_4S_3^-$	0.518 (0.667)	0.426 (0.679)			0.446 (0.506)				0.240 (0.382)
7	Cu_5S_4	0.533 (0.704)	0.523 (0.661)			0.353 (0.554)				
i-7[a]	$Cu_5S_4^-$	0.532 (0.599)	0.543 (0.601)			0.547 (0.604)				
8	$Cu_6S_4^-$	0.570 (0.633)	0.571 (0.585)							

[a] The new clusters found. [b] The values in parentheses were obtained at the MP2(FC)/6-311+G(d) level.

In the $(Cu_2S)_n$ clusters this ratio is 2:1 whereas in the case of the $Cu_xS_y^-$ species it is 1.5:1 or less. This difference generally leads to different coordination of atoms in the two groups of clusters. For example, in the species with two sulfur atoms, the coordination of sulfur in CuS_2^- and $Cu_2S_2^-$ changes from 1 to 2, whereas in the neutral Cu_4S_2 systems the coordination can be 3 and 4. Nevertheless, there are few Cu−S and Cu−Cu bonds that have similar coordination in the $Cu_xS_y^-$ and $(Cu_2S)_n$ clusters. On the basis of the values of $\rho(r_c)$, the strength of bonds to atoms that exhibit identical degrees of coordination are similar in the $Cu_xS_y^-$ and $(Cu_2S)_n$ clusters. For example, for $Cu_4S_3^-$ the value of $\rho(r_c)$ at the Cu2−S2 BCP is 0.45 e Å^{-3}. A similar value of 0.48 e Å^{-3} is found for the Cu−S bond of **2** (Cu_2S_4).[14] Comparable values of $\rho(r_c)$ are found at BCPs of similar Cu−Cu bonds. For example the value of $\rho(r_c)$ at the Cu2−Cu2′ BCP of $Cu_4S_3^-$ is 0.24, and the value found for analogous Cu−Cu bonds of two $(Cu_2S)_2$ clusters (structures **2** and **3** of ref 14) is 0.34.

We found three new structures not considered by Dance and co-workers.[15,16] One, **i-4**, is an isomer of $Cu_2S_3^-$ and the others, **i-5** and **i-7**, are isomers of **5** and **7**, respectively. They are displayed in Figures 2−4. While all Cu−S bonds shown in the graphical structures reported by Dance are recovered in the AIM analysis, many Cu−Cu bonds are not. It is possible that the differences arise from the variations in the geometries of the clusters obtained at different levels of theory and basis sets. Our previous study[14] on copper(I) sulfide $(Cu_2S)_n$ clusters showed that covalent bonding between Cu atoms is determined by the electron density distribution rather than by interatomic distances. In fact many of the Cu−Cu internuclear distances calculated by both Becke3PW91 and MP2 methods that do not exhibit covalent bonding are less than "normal" Cu−Cu bond distance of 2.65−2.70 Å,[27] for example: (a) Cu1−Cu1′ of **i-4** (i-$Cu_2S_3^-$), **5** (Cu_3S_3), **i-5** (i-$Cu_3S_3^-$), **6** ($Cu_4S_3^-$), and **7** ($Cu_5S_4^-$); (b) Cu1−Cu2 of **5** ($Cu_3S_3^-$), **7** ($Cu_5S_4^-$); (c) Cu1−Cu3 of **i-7** (i-$Cu_5S_4^-$). We checked the effect of varying the

TABLE 3: Values of $\nabla^2\rho(r_c)$ (e Å^{-5}) at Bond Critical Points

cluster		S1−Cu1	Cu1−S2	S1−S2	S1−Cu2	S2−Cu2	Cu1−Cu1′	Cu1−Cu2	Cu3−Cu1	Cu2−Cu2′
1	CuS_2^-	−1.164 (−1.201)[b]								
2	CuS_3^-	−1.182 (−1.341)		−0.099 (−0.056)						
3	$Cu_2S_2^-$	−0.987 (−1.024)					−0.023			
4	$Cu_2S_3^-$	−1.468 (−1.894)	−1.610 (−1.747)							
i-4[a]	$Cu_2S_3^-$	−1.062 (−1.175)	−1.195 (−1.495)	−0.485 (−0.032)			(−0.589)			
5	$Cu_3S_3^-$	−1.673 (−1.482)	−1.637 (−1.507)			−1.673 (−1.482)				
i-5[a]	$Cu_3S_3^-$	−1.378 (−1.621)	−1.127 (−1.332)		−0.702 (−0.796)	−0.816 (−0.683)				
6	$Cu_4S_3^-$	−1.200 (−1.506)	−1.107 (−1.263)			−0.730 (−0.924)				−0.647 (−0.646)
7	$Cu_5S_4^-$	−1.366 (−1.484)	−1.210 (−1.260)			−1.144 (−1.023)				
i-7[a]	$Cu_5S_4^-$	−1.117 (−1.276)	−1.006 (−1.094)			−1.018 (−1.115)				
8	$Cu_6S_4^-$	−1.013 (−1.143)	−1.016 (−1.123)							

[a] The new clusters found. [b] The values in parentheses were obtained at the MP2(FC)/6-311+G(d) level.

calculation method on geometry and molecular structure by comparing results obtained at the Becke3PW91/6-311+G(d), and MP2(FC)/6-311+G(d) levels. The molecular structures calculated by these two methods were identical except in two cases; $Cu_2S_2^-$ (Figure 1, parts c and d) and i-$Cu_2S_3^-$ (Figure 2, parts b and c). There is a bond path (BP) between Cu1 and Cu1′ of $Cu_2S_2^-$ at Becke3PW91 (Figure 1c) but not at the MP2(FC)/6-311+G(d) level (Figure 1d). In the case of **i-4** there is a BP between Cu1 and Cu1′ at the MP2(FC)/6-311+G(d) level (Figure 2c), but not at Becke3PW91 (Figure 2b). The tenuous nature of these bonds was indicated by the proximity of the RCPs (yellow) to the BCPs (red) and close values of $\rho(r_c)$ at these points. For example the values of $\rho(r_c)$ of $Cu_2S_2^-$ calculated with Becke3PW91 at BCP for Cu1−Cu1′ bond and at the adjacent RCP are 0.313 and 0.312 e Å^{-3} respectively; for i-$Cu_2S_3^-$ the values of $\rho(r_c)$ at the BCP and RCP at the MP2 level are also virtually identical at 0.406 and 0.404 e Å^{-3}, respectively. That the electron density distribution is quite flat at closely located BCPs and RCPs is supported by the eigenvalues of the Hessian (curvatures). For example, for $Cu_2S_2^-$, the eigenvalues at BCP of the Cu1−Cu1′ bond are −0.861, −0.133, and 3.254 and those at the RCP nearby are −0.838, 0.253, 2.876 e Å^{-5}; the curvature of electron density distribution along the geometrical line connecting S1 and S1′ changes little from the maximum at BCP ($\lambda_2 = -0.133$) to a minimum at RCP ($\lambda_2 = 0.253$) indicating the near degeneracy of these critical points.[25] This is also the case for the Cu1−Cu1′ BCP and the neighboring RCP of $Cu_2S_3^-$ (Figure 2(c)). At the BCP the curvatures are −1.198, −0.441, and 3.996 and at the RCP −1.120, 0.499, and 3.139. In such cases, a small increase in internuclear distance or decrease in the density between the copper atoms would result in the annihilation of the RCPs and BCPs. Thus the calculation method affects the geometry and molecular structure of $(Cu_xS_y)^-$ clusters only to a minor degree. We also carried out a limited study to ascertain the impact of basis set size on the geometry and molecular structure by carrying out calculations on $Cu_4S_3^-$ (**6**) at a lower level, MP2(FC)/6-31G(d). Significant changes in the molecular geometry are seen in going from MP2(FC)/6-311+G(d) to MP2(FC)/6-31G(d): Cu1−S1 increased from 2.133 to 2.149 Å, Cu1−S2 decreased from 2.127 to 2.068 Å, Cu1−Cu1′ decreased from 2.532 to 2.273 Å, and Cu1−Cu2 decreased from 2.678 to 2.358 Å. The molecular graphs displayed in Figure 3 as parts c and d show the results of the decreasing the Cu−Cu distances by 0.26 and 0.33 Å; respectively. BPs are found between the copper atoms at the MP2(FC)/6-31G(d) level but not at MP2(FC)/6-311+G(d)). The molecular graph of **6** at the Becke3PW91/6-311+G(d) is identical to the one obtained at the MP(FC) level displayed as Figure 3c. It is clear that basis set size is important, and this is in keeping with our earlier findings;[14] we showed that internuclear distances calculated for $(Cu_2S)_n$ clusters with the 6-311+G(d) basis set show better agreement with experimental data than the values obtained at the 6-31G(d) level. Even though substantially shorter Cu−Cu interatomic distances are calculated at the 6-31G(d) level for **6**, the covalent bonds are fragile. The curvatures are −1.708, −1.140, and 7.054 e Å^{-5} at the Cu1−Cu1′ BCP and −1.527, 1.537, and 5.150 e Å^{-5} at the closely positioned RCP. Curvatures of this type are characteristic of weak hydrogen or van der Waals bonds rather than covalent bonds. For example the values for the hydrogen bond of $(HF)_2$ are −0.978, −0.868, and 4.805 e Å^{-5}.[25] In contrast, the curvatures at the Cu1−S1 BCP of $Cu_4S_3^-$ (Figure 3d) are −3.108, −3.071, and 10.190 e Å^{-5}.

Table 4 lists the total and relative energies of the $(Cu_xS_y)^-$ clusters calculated with both methods along with the symmetries of the species. At the Becke3PW91/6-311+G(d) level we find two isomers, i-$Cu_2S_3^-$ (**i-4**) and i-$Cu_5S_4^-$ (**i-7**), that are more stable than **4** and **7**.[15] At the Becke3PW91/6-311+G(d) level the third new isomer i-$Cu_3S_3^-$ (**i-5**) is slightly less stable by +1.1 kcal mol^{-1} than **5**. To test the accuracy of these results we obtained data by averaging the MP3(FC)/6-311+G(d) and MP4(FC)/6-311+G(d) energies calculated using the MP2(FC)/6-311+G(d) geometries. As seen from Table 4, the relative stability of two new isomers calculated by MP2, MP3, and MP4(SDQ) not surprisingly depends on the order of perturbation correction. Our new cluster **i-5** is less stable than **5** at MP2 and MP4(SDQ) but more stable at MP3. Our new cluster **i-7** is less stable than **7** at MP2 but more stable at MP3 and MP4(SDQ) levels. Cluster **i-7** is also more stable than **7** at Becke3PW91. It is well-known that the MP2 correction overestimates the effect of electron correlation[28] and sometimes leads to incorrect results.[29] For “well-behaved” systems where HF, MP2, MP3, and MP4 energies show a monotonic convergence toward some asymptotic value, the correct answer must be somewhere

TABLE 4: Total and Relative Energies of $(Cu_xS_y)^-$ Clusters

cluster	sym	E_{T}[a]	E_{rel}[b]	E_{T}[a]				E_{rel}[b]
		(B3PW91)	(B3PW91)	MP2	MP3	MP4[c]	(MP3 + MP4)/2	(MP3 + MP4)/2
1 CuS_2^-	D^{*}_{h}	−2436.862369		−2434.707460	−2434.554159	−2434.695377	−2434.624768	
2 CuS_3^-	C_s	−2835.075296		−2832.376263	−2832.292524	−2832.381418	−2832.336971	
3 $Cu_2S_2^-$	C_{2v}	−4077.420738		−4073.839400	−4073.767531	−4073.829396	−4073.798463	
4 $Cu_2S_3^-$	C_2	−4475.561216	+38.0	−4471.695305	−4471.472426	−4471.695213	−4471.583819	+25.9
i-4[d] $Cu_2S_3^-$	C_s	−4475.621796	0.0	−4471.756968	−4471.524741	−4471.725491	−4471.625116	
5 $Cu_3S_3^-$	C_s	−6116.141045	0.0	−6111.162924	−6110.734172	−6111.096538	−6110.915355	+9.3
				−6112.866025[e]	−6112.029359[e]	−6112.805474[e]	−6112.417416[e]	+4.9[e]
i-5[d] $Cu_3S_3^-$	C_s	−6116.139264	+1.1	−6111.113664	−6110.799099	−6111.061122	−6110.930110	0.0
				−6112.811353[e]	−6112.113930[e]	−6112.736591[e]	−6112.425260[e]	0.0
6 $Cu_4S_3^-$	C_{2v}	−7756.693456		−7750.507660	−7750.057092	−7750.437358	−7750.247225	
7 $Cu_5S_4^-$	C_{2v}	−9795.424134	+21.4	−9787.637516	−9786.946568	−9787.485580	−9787.216074	+39.7
i-7[d] $Cu_5S_4^-$	C_{2v}	−9795.458299	0.0	−9787.614516	−9787.040942	−9787.517799	−9787.279371	0.0
8 $Cu_6S_4^-$	C_1	−11436.018807		−11426.939497	−11426.301547	−11426.822951	−11426.562249	

[a] Total energy in atomic units (hartrees). [b] Relative energy in kcal mol^{-1}. [c] At the MP4(SDQ)(FC) level unless stated otherwise. [d] The new clusters found. [e] MPN energies with all-electron (FULL) calculations.

between MP3 and MP4.[28] This is the rational for using the average of the MP3 and MP4 energies to obtain the most accurate relative energies. The results are listed in column nine while the Becke3PW91/6-311+G(d) results are shown in column four of Table 4. The MP3/MP4(SDQ) analysis also places **i-5** 9.3 kcal mol^{-1} lower in energy than **5**. We also checked the influence of including core shell electrons on the accuracy of our calculations by performing single-point full-electron MP3 and MP4(SDQ)/6-311+G(d) calculations on **5** and **i-5** with the MP2(FC)/6-311+G(d) geometries. Although the absolute values of the total energies differ from those obtained at the frozen core level (see columns five to nine of Table 4), the average of the MP3(FULL) and MP4(SDQ)(FULL) energies of **i-5** is still lower than the average value for **5** by 4.9 kcal mol^{-1}. On this basis, the new isomers **i-4**, **i-5**, and **i-7** are more stable than **4**, **5**, and **7** reported in ref 16.

Support for these results is provided by gas-phase collision induced dissociation (CID) studies on the $(Cu_xS_y)^-$ clusters with argon and tetrachloride carried out by Dance and co-workers.[15] One of the main products of dissociation of the $Cu_2S_3^-$ ion is S_2. If the most stable isomer was **4** then to make S_2, two Cu−S bonds must be broken and two S atoms combined to form S_2. At the high energy of the experiment (82 eV), association of two S atoms to form S_2 is unlikely. On the other hand, extrusion of S_2 from **i-4** would occur in a straightforward manner. Moreover, on the basis of the $\rho(r_c)$ values of (see column three of Table 2) the Cu1−S2 bonds of **4** are stronger than Cu1−S2 of **i-4**. It is also interesting to note that $\rho(r_c)$ for the S−S bond of **i-4** is higher than $\rho(r_c)$ of Cu1−S2, an indication that cleavage of Cu1−S2 bond could lead the extrusion of S_2. CID of $Cu_3S_3^-$ also yields S_2 as a product. If **5** were the structure of $Cu_3S_3^-$, then four strong Cu−S bonds must be cleaved and two S atoms combined to yield S_2. While four Cu−S bonds must also be broken in **i-5** as well, two of the four Cu−S bonds are weaker than those in the **5** (see columns four and seven, Table 2). CID of $Cu_5S_4^-$ also yields S_2 as a product; the arguments used in the case of **4**, **i-4**, **5**, and **i-5** apply to **7** and **i-7** as well. Further support for **i-7** is found in the CID results. Cluster $Cu_6S_4^-$ (**8**) yields $Cu_5S_4^-$ (**i-7**), which is easily formed from **8** by the extrusion of a Cu atom.

The new clusters **i-5** and **i-7** now provide a consistent picture of the reactivity of $(Cu_xS_y)^-$ anions with P_4 and triphenylphosphine[15,16] based on degree of coordination of sulfur atoms; **i-5**, **i-7**, and **8** possess a higher sulfur coordination than the reactive species **1**, **2**, **3**, **i-4**, and **6**. All sulfur atoms of the clusters that exhibit low reactivity or are nonreactive are three-coordinate. In $Cu_4S_3^-$ that exhibits low reactivity, two of three sulfurs are three-coordinate but one is two-coordinate. In the reactive clusters, the sulfur atoms are two-coordinated or less. According to the CID experiments, the main products of $Cu_2S_3P_2^-$ and $Cu_2S_2P_2^-$ decay are P_2S^- and PS_2^-, demonstrating that phosphorus prefers to bind to sulfur. The coordination number of sulfur is not limited to three since it has a valence shell configuration of s^2p^4. For example in bulk mineral chalcocite the sulfur atom of Cu_2S can coordinate to six neighbors.[30] However for small neutral stable clusters $(Cu_2S)_n$ in the gaseous phase, it was shown that the stabilization energy reaches saturation when sulfur reaches a coordination of four.[12,13] Stable $(Cu_xS_y)^-$ ions studied experimentally by combination of laser ablation and Fourier transform ion−cyclotron−resonance mass spectroscopy—except for the smallest ones—also have a clear tendency to keep the ratio of number of Cu and S atoms close to 2:1.[15] This is the case even for large clusters studied experimentally—up to $Cu_{45}S_{23}^-$—that have general formula $Cu_{2n-1}S_n$ or $Cu_{2n-2}S_n$. The stability of $(Cu_2S)_n$ clusters undoubtedly depends largely on sulfur coordination.[14]

Conclusions

Ab initio Becke3PW91/6-311+G(d), MPN(FC)/6-311+G(d), and MPN(FULL)/6-311+G(d) calculations along with AIM analyses can be used to study the molecular structure and stability of small $(Cu_xS_y)^-$ anionic clusters. Metal−metal covalent bonding is weak, unstable, and often not realized, even though interatomic distances are found to be within the normal Cu−Cu range. While all Cu−S covalent bonds assumed previously are confirmed by AIM analysis, many of the Cu−Cu bonds are not. An increase of basis set size from 6-31G(d) to 6-311+G(d) leads to an increase of Cu−Cu distances and a loss of tenuous covalent Cu−Cu bonds. A change in method from Becke3PW91 to MPN affects the geometry and molecular structure of $(Cu_xS_y)^-$ clusters only to a minor extent. Three new stable clusters have been found, nicely providing a connection between reactivity of $(Cu_xS_y)^-$ ions with P_4 and coordination of sulfur atoms in clusters. The reactive species have a lower coordination of the sulfur atoms (to which phosphorus binds) than nonreactive ones.

Acknowledgment. We thank the Shared Hierarchical Academic Research Computing Network of Ontario (SHARCNET) for providing computing resources at McMaster University. We gratefully acknowledge financial support by the Natural Sciences and Engineering Research Council of Canada (NSERC).

References and Notes

(1) Rees, D. C. *Annu. Rev. Biochem.* **2002**, *71*, 221.

(2) Alvarez, M. L.; Ai, J.; Zumft, W.; Sanders-Loehr, J.; Dooley, D. M. *J. Am. Chem. Soc.* **2001**, *123*, 576.

(3) Bae, W.; Mehra, R. K. *J. Inorg. Biochem.* **1998**, *70*, 125.

(4) Rasmussen, T.; Berks, B. C.; Sanders-Loehr, J.; Dooley, D. M.; Zumft, W. G.; Thomson, A. J. *Biochemistry* **2000**, *39*, 12753.

(5) Cardoso, J.; Gomez-Daza, O.; Ixtlilco, L.; Nair, M. T. S.; Nair, P. K. *Modern Phys. Lett. B* **2001**, *15*, *17*, *18 and 19*, 774.

(6) Godovsky, D. Y. *Adv. Polym. Sci.* **2000**, *153*, 163.

(7) Grozdanov, I.; Barlingay, C. K.; Dey, S. K. *Mater. Lett.* **1995**, *23*, 181.

(8) Nair, P. K.; Cardoso, J.; Gomez Daza, O.; Nair, M. T. S. *Thin Solid Films* **2001**, *401*, 243.

(9) Wang, S.; Yang, S.; Dai, Z. R.; Wang, Z. L. *Chem. Mater.* **2001**, *13*, 4794.

(10) Wang, S.; Yang, S. *Phys. Chem. Chem. Phys.* **2001**, *3*, 3750.

(11) Dehnen, S.; Eichhofer, A.; Fenske, D. *Eur. J. Inorg. Chem.* **2002**, 279.

(12) Eichorn, K.; Dehnen, S.; Ahlrichs, R. *Chem. Phys. Lett.* **1998**, *284*, 287.

(13) Dehnen, S.; Schafer, A.; Ahlrichs, R.; Fenske, D. *Chem.—Eur. J.* **1996**, 429.

(14) Ni, B.; Kramer, J. R.; Werstiuk, N. H. *J. Phys. Chem. A* **2003**, in press.

(15) Fisher, K.; Dance, I.; Willet, G.; Yi, M. N. *J. Chem. Soc., Dalton Trans.* **1996**, 709.

(16) Fisher, K.; Dance, I. *J. Chem. Soc., Dalton Trans.* **1997**, 2381.

(17) Fisher, K.; Dance, I.; Willett, G. *Polyhedron* **1997**, *16*, 2731.

(18) Frisch, M. J.; Trucks, G. W.; Schlegel, H. B.; Scuseria, G. E.; Robb, M. A.; Cheeseman, J. R.; Zakrzewski, V. G.; Montgomery, J. A.; Stratmann, R. E.; Burant, J. C.; Dapprich, S.; Millam, J. M.; Daniels, A. D.; Kudin, K. N.; Strain, M. C.; Farkas, O.; Tomasi, J.; Barone, V.; Cossi, M.; Cammi, R.; Mennucci, B.; Pomelli, C.; Adamo, C.; Clifford, S.; Ochterski, J.; Petersson, G. A.; Ayala, P. Y.; Cui, Q.; Morokuma, K.; Malick, D. K.; Rabuck, A. D.; Raghavachari, K.; Foresman, J. B.; Cioslowski, J.; Ortiz, J. V.; Stefanov, B. B.; Liu, G.; Liashenko, A.; Piskorz, P.; Komaromi, I.; Gomperts, R.; Martin, R. L.; Fox, D. J.; Keith, T.; Al-Laham, M. A.; Peng, C. Y.; Nanayakkara, A.; Gonzalez, C.; Challacombe, M.; Gill, P. M. W.; Johnson, B. G.; Chen, W.; Wong, M. W.; Andres, J. L.; Head-Gordon, M.; Replogle, E. S.; Pople, J. A. *Gaussian 98*, revision A.9; Gaussian, Inc.: Pittsburgh, PA, 1998.

(19) Perdew, J. P.; Wang, Y. *Phys. Rev. B* **1992**, *45*, 13244.

(20) Moller, C.; Plesset, M. S. *Phys. Rev.* **1934**, *46*, 618.

(21) Wilson, S. *Adv. Chem. Phys.* **1987**, *67*, 474.

(22) HyperChem. Copyright 1996, Hypercube, Inc.

(23) Biegler-Konig, F. W.; Bader, R. F. W.; Tang, T.-H. *J. Comput. Chem.* **1982**, *3*, 317.

(24) Biegler-Konig, F. AIM 2000. Copyright 1998−2000, University of Applied Science: Bielefeld, Germany.

(25) Bader, R. F. W. *Atoms in Molecules*; Oxford Science Publications: Oxford, U.K., 1990.

(26) Gibbs, G. V.; Boisen, M. B.; Beverly, L. L.; Rosso, K. M. *Rev. Mineral. Geochem.* **2002**, *42*, 345.

(27) Schafer, A.; Ahlrichs, R. *J. Am. Chem. Soc.* **1994**, *116*, 10686.

(28) Jensen, F. *Introduction to Computational Chemistry*; John Wiley & Sons Ltd.: London, 1999.

(29) Siegbahn, P. E. M. *Adv. Chem. Phys.* **1996**, *93*, 365.

(30) Evans, H. T., Jr. *Nature: Phys. Sci.* **1971**, *232*, 89.